Title

Post-translational modifications of soluble α-synuclein regulate the amplification of pathological α-synuclein.

Journal

Nature neuroscience, 26(2)

ISSN

1097-6256

Authors

Zhang, Shujing
Zhu, Ruowei
Pan, Buyan
et al.

Publication Date

2023-02-01

DOI

10.1038/s41593-022-01239-7

Peer reviewed

HHS Public Access

Author manuscript

Nat Neurosci. Author manuscript; available in PMC 2023 April 14.

Published in final edited form as:

Nat Neurosci. 2023 February ; 26(2): 213–225. doi:10.1038/s41593-022-01239-7.

Post-translational modifications of soluble α-synuclein regulate the amplification of pathological α-synuclein

Shujing Zhang[1,15], **Ruowei Zhu**[1,15], **Buyan Pan**[2], **Hong Xu**[3], **Modupe F. Olufemi**[3], **Ronald J. Gathagan**[3], **Yuanxi Li**[1,4,5], **Luyan Zhang**[1], **Jasmine Zhang**[1], **Wenxuan Xiang**[1], **Eliot Masahiro Kagan**[1], **Xingjun Cao**[6], **Chaoxing Yuan**[7], **Soo-Jung Kim**[3], **Christopher K. Williams**[8], **Shino Magaki**[8], **Harry V. Vinters**[9], **Hilal A. Lashuel**[10], **Benjamin A. Garcia**[11], **E. James Petersson**[2], **John Q. Trojanowski**[3], **Virginia M.-Y. Lee**[3], **Chao Peng**[1,12,13,14]

[1]Department of Neurology, David Geffen School of Medicine, University of California—Los Angeles, Los Angeles, CA, USA.

[2]Department of Chemistry, School of Arts and Sciences, University of Pennsylvania, Philadelphia, PA, USA.

[3]The Department of Pathology and Laboratory Medicine, Institute on Aging and Center for Neurodegenerative Disease Research, the Perelman School of Medicine, University of Pennsylvania, Philadelphia, PA, USA.

[4]Institute for Cognitive Neurodynamics, East China University of Science and Technology, Shanghai, China.

[5]School of Mathematics, East China University of Science and Technology, Shanghai, China.

[6]Innovent Biologics, Inc., Suzhou, China.

[7]Alexion Pharmaceuticals, Inc., New Haven, CT, USA.

[8]Section of Neuropathology, Department of Pathology and Laboratory Medicine, Ronald Reagan UCLA Medical Center and David Geffen School of Medicine, University of California—Los Angeles, Los Angeles, CA, USA.

Correspondence and requests for materials should be addressed to Virginia M.-Y. Lee or Chao Peng. vmylee@upenn.edu; cpeng@mednet.ucla.edu.

Author contributions

C.P., V.L., S.Z. and R.Z. conceived experiments. C.P., S.Z. and R.Z. performed most of the experiments. B.P. and E.J.P. generate pY39 and pS87 α-synuclein monomer. H.X., M.F.O., R.J.G., J.Z., W.X. and E.M.K. performed cell culture experiments. L.Z. and H.A.L. performed biochemical experiments. S.-J.K. generated PFF. C.K.W., S.M. and H.V. identified and prepared human brain tissue for the preparation of pathological α-synuclein. X.C., C.Y. and B.A.G. performed LC–MS/MS experiments. Y.L. analyzed the data. C.P., J.Q.T., V.M.-Y.L., E.J.P. and H.A.L. wrote the manuscript.

Online content

Any methods, additional references, Nature Portfolio reporting summaries, source data, extended data, supplementary information, acknowledgements, peer review information; details of author contributions and competing interests; and statements of data and code availability are available at https://doi.org/10.1038/s41593-022-01239-7.

Reporting summary

Further information on research design is available in the Nature Portfolio Reporting Summary linked to this article.

Competing interests

The authors declare no competing interests.

Supplementary information The online version contains supplementary material available at https://doi.org/10.1038/s41593-022-01239-7.

[9]Section of Neuropathology, Department of Pathology and Laboratory Medicine, Department of Neurology, and Brain Research Institute, Ronald Reagan UCLA Medical Center and David Geffen School of Medicine, University of California – Los Angeles, Los Angeles, CA, USA.

[10]Laboratory of Molecular and Chemical Biology of Neurodegeneration, Brain Mind Institute, Swiss Federal Institute of Technology, Lausanne, Switzerland.

[11]Department of Biochemistry and Molecular Biophysics, Washington University St Louis, St Louis, MO, USA.

[12]Molecular Biology Institute, University of California, Los Angeles, California, Los Angeles 90095, USA.

[13]Brain Research Institute, University of California, Los Angeles, Los Angeles, California, 90095, USA.

[14]Mary S. Easton Center for Alzheimer's Research, University of California, Los Angeles, Los Angeles, California 90095, USA.

[15]These authors contributed equally: Shujing Zhang, Ruowei Zhu.

Abstract

Cell-to-cell transmission and subsequent amplification of pathological proteins promote neurodegenerative disease progression. Most research on this has focused on pathological protein seeds, but how their normal counterparts, which are converted to pathological forms during transmission, regulate transmission is less understood. Here we show in cultured cells that phosphorylation of soluble, nonpathological α-synuclein (α-Syn) at previously identified sites dramatically affects the amplification of pathological α-Syn, which underlies Parkinson's disease and other α-synucleinopathies, in a conformation- and phosphorylation site-specific manner. We performed LC–MS/MS analyses on soluble α-Syn purified from Parkinson's disease and other α-synucleinopathies, identifying many new α-Syn post-translational modifications (PTMs). In addition to phosphorylation, acetylation of soluble α-Syn also modified pathological α-Syn transmission in a site- and conformation-specific manner. Moreover, phosphorylation of soluble α-Syn could modulate the seeding properties of pathological α-Syn. Our study represents the first systematic analysis how of soluble α-Syn PTMs affect the spreading and amplification of pathological α-Syn, which may affect disease progression.

α-Synucleinopathies are a group of neurodegenerative diseases characterized by the intracellular accumulation of pathological α-Syn. These include Parkinson's disease, dementia with Lewy bodies, multiple system atrophy (MSA) and ~50% of Alzheimer's disease cases[1-3]. During the past decades, mounting evidence supports cell-to-cell transmission and subsequent amplification of pathological α-synuclein (α-Syn) as a key process for the onset and progression of α-synucleinopathies[4-7]. Tremendous efforts have been spent exploring the molecular mechanisms that modulate the transmission process. Particularly, the release, uptake, transport and degradation of pathological α-Syn seeds have been extensively investigated in multiple studies[8,9]. However, successful amplification of the pathological protein involves two components, the formation of pathological α-Syn seeds and the transformation of normal, soluble α-Syn, that is, the substrate. The potential

regulatory role played by soluble α-Syn in the amplification of pathological α-Syn has not yet been investigated.

Numerous post-translational modifications (PTMs) have been identified in α-Syn[10,11] and were shown to modulate the aggregation and clearance of monomeric α-Syn in vitro[12-18]. Even though previous studies of α-Syn PTMs have been focused more on pathological α-Syn, multiple PTMs, particularly phosphorylation, have also been identified on soluble α-Syn prepared from normal brains[16,18-20]. We hypothesize that PTMs in soluble α-Syn could modulate the interaction between pathological α-Syn and soluble α-Syn, which in turn could regulate the amplification of pathological α-Syn and modulate the α-Syn aggregate transmission process.

In this Article, we evaluated the effect of soluble α-Syn phosphorylation at known sites on the amplification of pathological α-Syn. Phosphorylation of soluble α-Syn dramatically affected the amplification of pathological α-Syn. Interestingly, this effect is phosphorylation site and conformation dependent. Different phosphorylation sites have distinct effects on the same pathological α-Syn strain, and the same phosphorylation sites could have distinct effects on different pathological α-Syn strains, highlighting for the first time the complex interaction between soluble α-Syn phosphorylation sites and different pathological α-Syn conformations. Because previous studies of α-Syn PTMs have focused more on pathological α-Syn and fewer studies have been performed to explore PTMs on soluble α-Syn, LC–MS/MS was used to systematically identify PTMs in soluble α-Syn purified from various α-synucleinopathies. Notably, soluble α-Syn is acetylated and this acetylation of soluble α-Syn also modulated the amplification of pathological α-Syn in a strain-dependent way, thereby demonstrating that the observed effects are not restricted to phosphorylation. Finally, by passaging pathological α-Syn with different phosphorylation mimics, we demonstrated that PTMs in soluble α-Syn could also modulate the property of the original seeds after passaging. Therefore, soluble α-Syn PTMs represent a critical new mechanism that modulates the transmission of pathological α-Syn.

Results

Soluble α-Syn phosphorylation modulates the amplification of pathological α-Syn

To explore whether phosphorylation of soluble α-Syn modulates the amplification of pathological seeds and regulates the transmission process, we first confirmed the existence of several previously reported α-Syn phosphorylation sites, that is, serine 87 (S87) and tyrosine 39 (Y39) on soluble α-Syn[16,18]. Consistent with previous reports[16,18], both phosphorylated S87 (pS87) and Y39 (pY39) soluble α-Syn were detected in both diseased and normal control brains (Supplementary Figs. 1, 2 and Supplementary Table 1). There was a dramatic variation in the amount of soluble pY39 or pS87 α-Syn in individual brains; however, no significant differences were observed among different α-synucleinopathies or compared to normal brains (Supplementary Figs. 1, 2 and Supplementary Table 1). Taking advantage of synthesized pY39 and pS87 α-Syn monomer, we evaluated the percentage of soluble α-Syn from diseased and control brains that is phosphorylated at Y39 or S87. About 10–40% of α-Syn proteins were phosphorylated at Y39, and 10–20% of α-Syn proteins were phosphorylated at S87, suggesting that there is a significant amount of

phosphorylated soluble α-Syn in diseased and control brains (Supplementary Fig. 3). To explore the nature of pY39 and pS87 α-Syn in diseased and normal brains, we resolved soluble α-Syn on native gels and found that a large amount (25–60%) of pY39 α-Syn is monomers (Supplementary Fig. 4). A reasonable amount (5–10%) of pS87 α-Syn monomers could also be detected (Supplementary Fig. 4).

To examine the effects of soluble α-Syn phosphorylation on the transmission of pathological α-Syn, we mutated Y39, S87, Y125 and Y133 to glutamic acid (E) to mimic the different phosphorylated α-Syn and expressed these variants α-Syn in HEK293 cells (Fig. 1a). Immunoblot analyses showed that various variant α-Syn had similar expression levels compared to the wild-type (WT) control (Fig. 1b,c). After transducing HEK293 cells with α-Syn preformed fibrils (PFFs), cells expressing different α-Syn variants were extracted with 1% Triton X-100 to remove soluble proteins and immunostained with a monoclonal antibody against α-Syn phosphorylated at S129 (81A) to evaluate the induction of α-Syn aggregation (Fig. 1d). Interestingly, none of the phosphorylation sites dramatically affected the seeding ability of α-Syn PFF (Fig. 1d,e).

α-Syn PFFs generated in test tubes have distinct conformations compared with pathological α-Syn prepared from Lewy body disease (LBD) brains (LB-α-Syn)[21,22]. To evaluate whether phosphorylation of soluble α-Syn could affect the seeding ability of pathological α-Syn isolated from diseased brains, HEK293 cells expressing different α-Syn phosphorylation variant mimics were transduced with LB-α-Syn prepared from LBD brains. Strikingly, Y39 phosphorylation dramatically blocked the seeding of soluble α-Syn by LB-α-Syn, in contrast to PFFs. S87 phosphorylation slightly increased, while Y125E and Y133 phosphorylation slightly reduced the seeding ability of LB-α-Syn, even though the effects were not as strong as those seen for Y39 phosphorylation (Fig. 1f,g and Supplementary Tables 2, 3). Interestingly, S87 phosphorylation has been shown to block α-Syn aggregation before[14,17], suggesting that the same phosphorylation site could have distinct roles during the initiation versus amplification of pathological α-Syn.

Due to the limited quantities of LB-α-Syn recovered from diseased brains that we were able to add to the HEK293 cells (4 ng per well), the amount of α-Syn pathology induced by LB-α-Syn was much lower than that induced by PFFs (40 ng per well) (Fig. 1d,f). To rule out any potential confounds resulting from low amounts of pathological α-Syn, HEK293 cells expressing α-Syn were transduced with the same amount of PFFs (4 ng per well) as LB-α-Syn. To mimic the contaminating proteins in the LB-α-Syn preparations, PFFs were mixed with insoluble proteins prepared from normal control brains. Even though all phosphorylation sites slightly reduced the seeding activity of low amounts of PFFs, no phosphorylation of soluble α-Syn dramatically affected the seeding ability of low amounts (4 ng per well) of PFFs (Fig. 1h and Supplementary Fig. 5), which is very different from LB-α-Syn. These data demonstrate that the LB-α-Syn and PFFs indeed show distinct responses to soluble α-Syn PTMs.

Previous studies, including ours, demonstrated that pathological α-Syn isolated from MSA patients, that is, GCI-α-Syn, has distinct conformations and seeding abilities compared with LB-α-Syn and PFFs[21-23]. To evaluate whether soluble α-Syn phosphorylation

would also affect the seeding ability of GCI-α-Syn, HEK293 cells expressing α-Syn phosphorylation mimicking variants were transduced with GCI-α-Syn. Interestingly, S87 phosphorylation dramatically blocked the seeding ability of GCI-α-Syn, which is in striking contrast to the increase seen with LB-α-Syn (Fig. 1i,j). Y39 phosphorylation also reduced the seeding of GCI-α-Syn. However, the effect was much weaker than for S87 phosphorylation. Y125 phosphorylation did not affect the amplification of GCI-α-Syn, and Y133 phosphorylation slightly reduced GCI-α-Syn amplification. These data again demonstrated that phosphorylation of soluble α-Syn affects the seeding ability of pathological α-Syn and this effect is conformation and phosphorylation site dependent. Comparing the effect of soluble α-Syn phosphorylation on different α-Syn strains from human α-Synucleinopathy brains showed that Y39 phosphorylation blocked the seeding ability of both LB-α-Syn and GCI-α-Syn and had no effect on PFFs. However, the effect is much stronger on LB-α-Syn than GCI-α-Syn (Fig. 1k). S87 phosphorylation increased the seeding ability of LB-α-Syn but dramatically blocked the seeding ability of GCI-α-Syn while having no obvious effect on PFFs (Fig. 1k).

To confirm that the pS129 α-Syn observed in HEK293 cells shown in Fig. 1 was indeed insoluble α-Syn, we extracted the transduced cells with 1% hexadecyltrimethylammonium bromide (HDTA) to remove all soluble α-Syn and stained the extracted cells with an antibody against total α-Syn. There was no signal in cells expressing α-Syn without transduction, which demonstrated the successful removal of all soluble α-Syn from the cells. Therefore, the stained total α-Syn in the transduced cells was indeed insoluble α-Syn (Supplementary Fig. 6a). Using this assay, we confirmed the effect of soluble α-Syn phosphorylation on pathological α-Syn amplification (Supplementary Fig. 6b-d). We also performed sequential extraction with 1% Triton X-100 and 1% Sarkosyl on HEK293 cells expressing different phosphorylation mimetic α-Syn variants and transduced with PFF or GCI-α-Syn. The resulting soluble and insoluble fractions were analyzed by western blot (WB) with an antibody against total α-Syn. The results further demonstrated the effect of soluble α-Syn phosphorylation on pathological α-Syn amplification (Supplementary Fig. 6e-h). Nonphosphorylation mimetic α-Syn variants (Y39A and S87A) do not affect the amplification of pathological α-Syn, demonstrating that the observed effect for phosphorylation mimetic variants is phosphorylation specific (Supplementary Fig. 7).

Because phosphorylation mimetic α-Syn variants dramatically modulate the amplification of LB-α-Syn and GCI-α-Syn, we further evaluated whether bona fide phosphorylation at the same residues could also modulate the amplification of pathological α-Syn. We first tested the effects of phosphorylation using a cell-free seeding assay. pY39 α-Syn and pS87 α-Syn monomers were generated using protein semi-synthesis strategies modified from previous approaches[24,25] and mixed at a ratio of 1:1 (95 ng μl^{-1} for each monomer). This pY39 and pS87 α-Syn monomer mixture was seeded with LB-α-Syn, GCI-α-Syn and PFF (10 ng μl^{-1}). After fibrilization, the amount of pY39 and pS87 α-Syn in the fibril fraction was analyzed by sedimentation assay and WB with anti-pY39 α-Syn and anti-pS87 α-Syn antibodies (Fig. 2a). We also confirmed that 95 ng μl^{-1} pY39 and pS87 α-Syn monomer mixture did not aggregate by themselves (Supplementary Fig. 8). Consistent with our observation for phosphorylation mimetic α-Syn variants, PFF seeded pY39 and pS87 α-Syn monomers equally well (Fig. 2b,e). However, LB-α-Syn preferentially seeded

pS87 α-Syn monomer (Fig. 2c,f), while GCI-α-Syn preferentially seeded pY39 monomer (Fig. 2d,g). Therefore, using pY39 and pS87 α-Syn monomers, we demonstrated that real phosphorylation on soluble α-Syn could also modulate the amplification of pathological α-Syn.

Previously, c-Abl has been shown to phosphorylate α-Syn on Y39 (ref. [16]), which provides an ideal tool to test the effect of pY39 on pathological α-Syn amplification in cells. We coexpressed c-Abl and WT α-Syn in HEK293 cells and demonstrated that c-Abl could efficiently phosphorylate α-Syn on Y39 (Fig. 2h,i). Notably, expressing α-Syn alone or coexpressing α-Syn with c-Abl showed similar levels of total α-Syn (Fig. 2j). HEK293 cells that express α-Syn alone or coexpress α-Syn with c-Abl were transduced with LB-α-Syn, GCI-α-Syn and PFF. Consistent with our observations for phosphorylation mimetic α-Syn variants, pY39 α-Syn generated in situ through c-Abl expression reduced the seeding activity of LB-α-Syn (Fig. 2m,n) and GCI-α-Syn (Fig. 2o,p) but did not have an obvious effect on the amplification of PFF α-Syn (Fig. 2k,l). Given the dramatic effect of soluble α-Syn phosphorylation on pathological α-Syn amplification, we further evaluated the amount of pY39 and pS87 α-Syn contained in GCI-α-Syn and LB-α-Syn. Indeed, there is less pY39 α-syn in LB-α-syn compared with GCI-α-syn, which is consistent with the observation that pY39 α-syn reduces the amplification of LB-α-syn more than GCI-α-syn (Supplementary Fig. 9a-c). However, we do not observe obvious differences between GCI-α-Syn and LB-α-Syn in terms of the amount of pS87 α-Syn (Supplementary Fig. 9d-f). This observation may be due to the fact that α-Syn could also be phosphorylated on Y39 and S87 by kinases or be dephosphorylated by phosphatases after aggregation. Therefore, the amount of pY39 and pS87 on pathological α-Syn might not always reflect the amount of pY39 and pS87 α-Syn monomer that is recruited during the amplification process.

Systematically identify PTMs on soluble α-Syn purified from diseased and control brains

Because soluble α-Syn phosphorylation could affect the seeding ability of pathological α-Syn, we asked if other types of PTMs would have similar effects. However, most previous studies of α-Syn PTMs have focused on defining modification sites on pathological α-Syn while the PTMs of soluble α-Syn have been less explored. To systematically analyze PTMs on soluble α-Syn, purified soluble α-Syn samples were generated from brains of various α-synucleinopathies and normal brains by immunoprecipitation (IP) and then analyzed by LC–MS/MS (Fig. 3a,b). To facilitate the identification of PTMs, multiple cases from each group were used and different LC–MS/MS methods were applied in these studies (Supplementary Tables 4 and 5). First, a single band of IP-purified α-Syn was excised and used for data-dependent LC–MS/MS analysis. Second, the entire preparation of IP-purified soluble α-Syn was used for data-dependent LC–MS/MS analysis. Third, cases with large quantities of pathological α-Syn or with particularly low postmortem intervals were selected for the study. Fourth, several samples were analyzed by LC–MS/MS for two continuous rounds, with the second run excluding the ions that were identified in the first run. Fifth, to facilitate the identification of phosphorylation and acetylation sites, parallel reaction monitoring was performed on samples enriched for phosphorylated and acetylated peptides. Finally, treatments with proteases such as trypsin and AspN were used to ensure coverage of the entire length of the α-Syn molecule. A total of 50 LC–MS/MS

analyses were performed. These data were analyzed for phosphorylation, acetylation, methylation, dimethylation, trimethylation, O-GlcNAc, 4-hydroxynonenal, oxidation of tyrosine, carboxymethyl, carboxyethyl, arginylation and ubiquitination. The results are summarized in Fig. 3c and Supplementary Tables 6-8. A total of 51 modifications were identified, with 44 of them being new modifications. 35 of 52 identified PTMs were located in the N-terminal domain. The most abundant modifications of soluble α-Syn were carboxymethylation, acetylation and methylation. Several new phosphorylation sites (S42, T64, T72, T75 and T81) were also identified. Finally, phosphorylation within the NAC domain (for example, T64, T72, T75 and T81) seems to be particularly enriched in soluble α-Syn isolated from MSA brains (Fig. 3c and Supplementary Tables 7, 8).

Soluble α-Syn acetylation also modulates the amplification of pathological α-Syn

Given the large number of new acetylation sites identified on soluble α-Syn, we asked if acetylation of soluble α-Syn could also modulate the transmission of pathological α-Syn. Lysine (K) to glutamine (Q) variants were used to mimic lysine acetylation. Different K to Q α-Syn variants have similar expression levels compared with WT Syn (Fig. 4a,b). Similar to phosphorylation, the different acetylation sites do not affect the seeding ability of PFFs dramatically, except for K43Q, which reduced the seeding ability of PFFs (Fig. 4c,d). K21 acetylation also slightly reduced the amplification of PFF. In contrast, different acetylation sites dramatically modulated the seeding of soluble α-Syn by LB-α-Syn with acetylation at K21, K43 and K45 dramatically reducing the seeding capacity of LB-α-Syn (Fig. 4e,f). K60 acetylation also slightly reduced the seeding capacity of LB-α-Syn. Furthermore, acetylation on soluble α-Syn also modulated the seeding ability of GCI-α-Syn dramatically, but with a very different pattern compared to LB-α-Syn because only K43 and K45 acetylation efficiently reduced the seeding ability of GCI-α-Syn (Fig. 4g,h). K21Q slightly reduced GCI-α-Syn amplification, but K60Q increased GCI-α-Syn amplification. We also compared the effects of soluble α-Syn acetylation on the seeding ability of different pathological α-Syn strains and demonstrated that K21, K45, K60 and K96 acetylation have differential effects on the transmission of different α-Syn strains (Fig. 4i), demonstrating that acetylation on soluble α-Syn also modulated the amplification of pathological α-Syn in a site and strain-dependent manner. We further confirmed the effect of soluble α-Syn acetylation on pathological α-Syn amplification by examining the amount of insoluble α-Syn induced by different pathological α-Syn strains in acetylation mimetic α-Syn variants (Supplementary Fig. 10). Nonacetylation α-Syn variants (K43A and K45A) do not affect the amplification of LB-α-Syn and GCI-α-Syn, demonstrating that observed effect is acetylation specific (Supplementary Fig. 11). Interestingly, K43A variant reduced the amplification of PFF α-Syn, suggesting that this residue is critical for PFF amplification (Supplementary Fig. 11).

The effect of soluble α-Syn is pathological α-Syn conformation dependent

Our prior studies showed that passaging GCI-α-Syn in primary neurons maintains its seeding ability and conformation[23] (Fig. 5a). Even after one round of passaging in primary neurons, more than 99% of the passaged GCI-α-Syn (GCI-N) are composed of mouse α-Syn[23]. Therefore, this system allows us to artificially generate an α-Syn strain with mouse α-Syn sequence but maintain the GCI-α-Syn conformation. This strain provided

us with a unique tool to ask if the effects of soluble α-Syn PTMs on GCI-α-Syn depend on the amino acid sequence or on its unique conformation. HEK293 cells expressing WT or various variant α-Syn were transduced with GCI-N and the induced α-Syn pathologies were analyzed and quantified (Fig. 5b-e). Notably, GCI-N showed a very similar response to soluble α-Syn acetylation and phosphorylation as GCI-α-Syn (Fig. 5f,g). These results demonstrate that the unique responses to soluble α-Syn PTMs of different pathological α-Syn strains are conformation dependent rather than sequence dependent.

Next, we asked if the effects of soluble α-Syn PTMs could be observed in primary neurons. In rat primary neurons, α-Syn is expressed at relatively low levels and it is hard to induce α-Syn pathology in these neurons using misfolded α-Syn seeds (Fig. 6c-f). However, infecting these cells with Adeno-associated viruses (AAVs) to express α-Syn could dramatically facilitate the induction of α-Syn pathology (Fig. 6c-f). Taking advantage of this expression system, we infected rat neurons with AAVs expressing WT or S87E variant α-Syn and transduced them with GCI-α-Syn, LB-α-Syn or α-Syn PFFs. This enabled us to ask if the effects of soluble α-Syn PTMs on transmission could be observed in primary neurons (Fig. 6a). WT and S87E variant α-Syn showed similar expression levels in primary neurons (Fig. 6b). Interestingly, while the S87E variant α-Syn showed no obvious effect on the seeding ability of α-Syn PFFs (Fig. 6c,d), it dramatically reduced the seeding ability of GCI-α-Syn (Fig. 6c,e) and increased the seeding ability of LB-α-Syn (Fig. 6c,f) compared with WT α-Syn, similar to what was observed in HEK293 cells. Thereby, this observation demonstrates that the effects of soluble α-Syn PTMs on pathological α-Syn amplification could also be observed in primary neurons.

Soluble α-Syn PTMs also modulate the seeding properties of pathological α-Syn

Finally, because we demonstrated that α-Syn PTMs could modulate the recruitment of soluble α-Syn by different α-Syn strains, we further asked whether PTMs on soluble α-Syn could also modulate the seeding properties of pathological α-Syn. In other words, will amplifying pathological α-Syn with α-Syn monomers carrying different PTMs change the seeding properties of the amplified pathological α-Syn? To answer this question, α-Syn PFFs and GCI-α-Syn were passaged in HEK293 cells expressing various α-Syn phosphorylation mimic variants. Then, the seeding ability of passaged PFFs and GCI-α-Syn was evaluated by transducing primary neurons (Fig. 7a). Strikingly, while phosphorylation on soluble α-Syn showed no obvious effect on PFFs, the Y39 and S87 phosphorylation variants dramatically reduced the seeding ability of GCI-α-Syn (Fig. 7b,c and Supplementary Fig. 12). Passaging GCI-α-Syn and PFFs in different α-Syn variants for two rounds showed that the expression of phosphorylation mimics Y39E and S87E further reduced the seeding ability of GCI-α-Syn (Fig. 7d,f and Supplementary Fig. 13). Interestingly, after passaging in different α-Syn variants for two rounds, S87 phosphorylation also dramatically reduced the seeding ability of PFFs (Fig. 7e and Supplementary Fig. 13). These results demonstrated that soluble α-Syn PTMs could not only affect the amplification of pathological α-Syn but also affect the seeding properties of pathological α-Syn after amplification.

In summary, our study demonstrates a previously unknown regulatory role of PTMs on soluble α-Syn in the transmission of pathological α-Syn. On the one hand, PTMs of soluble α-Syn dramatically modulate the interaction between soluble α-Syn and pathological α-Syn. Interestingly, this effect was both modification site and pathological α-Syn conformation dependent. Thus, the same PTM would have very different effects on different α-Syn strains. On the other hand, the amplification of pathological α-Syn with soluble α-Syn carrying different PTMs could also modulate the seeding property of the amplified pathological α-Syn. Finally, to further explore this regulatory network of PTMs on soluble α-Syn, we also systematically identified PTMs in soluble α-Syn of different α-Synucleinopathies by LC–MS/MS, which could be a critical resource for further studies.

Discussion

Transmission of pathological α-Syn along the central nervous system (CNS) is a shared mechanism for the progression of various neurodegenerative diseases. Prior studies of this process mainly focused on defining the behavior of pathological α-Syn (the seeds). However, successful amplification of the pathological α-Syn involves two components, the formation of pathological α-Syn seeds and the transformation of normal, soluble α-Syn, that is, the substrate. The potential regulatory role of the normal counterparts (soluble α-Syn) has generally been ignored. Here we showed for the first time that phosphorylation in soluble α-Syn dramatically modified the spreading of pathological α-Syn. Notably, this effect is pathological α-Syn conformation dependent. Using LC–MS/MS, we systematically identified the PTMs on soluble α-Syn purified from diseased and control brains. Then, we demonstrated that soluble α-Syn acetylation also modulates the amplification of pathological α-Syn in a conformation-dependent way. Finally, we found that soluble α-Syn could also modulate the seeding properties of pathological α-Syn. In summary, soluble α-Syn PTMs modulate the spreading of pathological α-Syn in two different ways. On the one hand, PTMs of soluble α-Syn could affect the recruitment of endogenous α-Syn by the pathological seeds. On the other hand, PTMs of soluble α-Syn could also modulate the seeding properties of pathological α-Syn once incorporated.

Previous studies by Lashuel and colleagues showed that phosphorylation of α-Syn monomers at S87 inhibits its aggregation in vitro and mimicking phosphorylation in vivo attenuates α-Syn aggregation and toxicity in rat models of α-synucleionpathies[18,26]. However, the phosphorylation at S87 slightly increased the amplification of LB-α-Syn, highlighting the different roles that PTMs have during the different stages of pathology development. Interestingly, S87 phosphorylation dramatically blocked the amplification of GCI-α-Syn and reduced the seeding capacity of GCI-α-Syn, suggesting that increasing phosphorylation at this site could be an attractive new drug target for MSA patients. On the other hand, tyrosine phosphorylation at Y39 has been shown to reduce α-Syn fibrilization in vitro[13] but was suggested to enhance the α-Syn aggregation in vivo[27]. In our study, we found that Y39 phosphorylation on soluble α-Syn could reduce the amplification of LB-α-Syn and GCI-α-Syn. Furthermore, Y39 phosphorylation dramatically reduces the seeding potency of amplified GCI-α-Syn, again suggesting that the same PTM can have different roles in different stages of disease pathogenesis.

Among the 11 different soluble α-Syn PTMs analyzed in the current study, seven PTMs could modulate the amplification of at least one of the pathological α-Syn strains, supporting that the regulation of transmission by soluble α-Syn is a very common phenomenon that is not restricted to a particular type of modification or specific modification site. However, among these seven PTMs, only one PTM (K43 acetylation) showed consistent effects on all three α-Syn strains (that is, LB-α-Syn, GCI-α-Syn and synthetic α-Syn PFFs), demonstrating that the effects of soluble α-Syn PTMs on transmission are highly selective to specific conformations. The fact that GCI-N and GCI-α-Syn showed similar responses to soluble α-Syn PTMs further demonstrated that the effects of PTMs on pathological α-Syn transmission are conformation rather than amino acid sequence dependent. Different pathological α-Syn strains show different spreading patterns in the CNS[23], but the underlying molecular mechanisms of these processes remain unknown. Our study indicates that the very distinct responses of different α-Syn strains to the same PTM could contribute to their different spreading patterns in the CNS and eventually contribute to the clinical diversity of different α-synucleinopathies.

To the best of our knowledge, our study represents the first systematic analysis of PTMs on soluble α-Syn. Previous studies of α-Syn PTMs were biased toward the PTMs on pathological α-Syn while our study identified a large number of new modifications in soluble α-Syn prepared from various diseased brains, which could be a critical resource for future studies on the biological functions of these modifications. The majority of the PTMs (34 of 51) were concentrated at the N-terminal domain. But five of the seven phosphorylation sites were found in the NAC domain. Four of these five phosphorylation sites have only been identified in soluble α-Syn prepared from MSA brains. Given the fact that S87 phosphorylation could only block the amplification of GCI-α-Syn, the enrichment of NAC domain phosphorylation such as S87 on soluble α-Syn from MSA patients could be a potential defense mechanism to reduce α-Syn transmission in MSA patients.

Previous studies suggested that acetylation on the N-terminal domain of α-Syn can block α-Syn aggregation[28]. Here we found that acetylation at different α-Syn sites shows differing effects on the amplification of LB-α-Syn and GCI-α-Syn. Overall, acetylation reduced the amplification of different α-Syn strains, suggesting that increasing the acetylation level on α-Syn could be beneficial for different α-Synucleinopathy patients. Previous studies have suggested that glycation promotes the aggregation of α-Syn[29]. We have identified multiple glycation sites on soluble α-Syn purified from diseased brains. It would be interesting to follow up on these glycation sites and study their role in the regulation of α-Syn transmission. O-GlcNAc on α-Syn has been reported to block α-Syn aggregation[15,30]. We have identified two O-GlcNAc sites on soluble α-Syn[29]. α-Syn arginylation has also been shown to block the aggregation of α-Syn[25,31,32]. We identified one arginylation site in soluble α-Syn from diseased brains. Methylation and dimethylation of α-Syn have not been studied before. However, we identified multiple new methylation and demethylation sites in soluble α-Syn, which could be an attractive new area to study.

In summary, our study illustrates a previously unknown regulatory role of soluble α-Syn on the transmission of pathological α-Syn. Given the high complexity of PTMs on soluble α-Syn and the complicated interaction between soluble α-Syn PTMs with pathological

α-Syn, this regulatory role of PTMs on soluble α-Syn could contribute substantially to the clinical and pathological landscape of diverse α-Synucleinopathies. Looking into the future, this effect of soluble α-Syn PTMs on pathological α-Syn spreading is worth further verification in animal models and also in patients. Notably, this idea of a regulatory role for soluble proteins could be easily expanded to other neurodegenerative diseases, such as tauopathies, because numerous PTMs have been identified on soluble tau[33] and various tau strains have been reported[34].

Methods

Statistics and reproducibility

The Investigators were blinded to the conditions of the experiments during data collection and quantification. No statistical methods were used to predetermine sample sizes but our sample sizes are similar to those reported in previous publications[23]. The normality and equal variances were formally tested for statistical analysis. Image Studio was used to collect the WB data. Accompanying software for IN Cell Analyzer 2200 was used to image the stained cells. Accompanying software for Molecular Devices Spectramax M5 plate reader was used to read the ELISA plates. Excel (Office 2019) was used to analyze the ELISA results. Cultured cells were equally assigned to each treatment group. Cell culture wells with server unexpected cell death (> 50% cell death compared with other groups) have been excluded from the analysis.

All statistical tests were two-tailed, and significance was assigned at $P < 0.05$. Normality was assessed by Shapiro–Wilk test. Equal variances between group samples were assessed by Brown–Forsythe test. One sample *t*-test (for normally distributed data) or one sample Wilcoxon test (for non-normally distributed data) was used for comparing the difference between variant groups and the WT group. Because they led to multiple comparisons, the false discovery rate (FDR) method was used for correcting the *P* values. Unpaired or paired *t*-test were used for comparing the differences between two groups, while Welch's correction was necessary if the variances had a significant difference. One-way ANOVA with Tukey's multiple comparison test was used for comparing the differences among multiple groups when the data followed normal distributions and no differences among the variances, while Kruskal–Wallis test with Dunn's multiple comparison test was used if the data were non-normally distributed. All the statistics were performed in Graphpad 8.0 (GraphPad Prism, GraphPad Software, www.graphpad.com) and R (The R Project for Statistical Computing (2022), available at https://www.R-project.org/).

Source of cell lines

The HEK293 is purchased from ATCC (CRL-1573).

Generation of α-Syn PFFs

α-Syn monomers and PFFs were generated as previously described in ref. [35]. Briefly, human WT or S87N α-Syn was expressed in BL21 (DE3) RIL cells and boiled in high-salt (HS_ buffer; 750 mM NaCl, 10 mM Tris (pH 7.6) and 1 mM EDTA). Then, α-Syn monomers were purified using Superdex 200 column (GE Healthcare Life Sciences) and a Hi-Trap

Q HP anion-exchange column (GE Healthcare Life Sciences) sequentially. Fibrillization was conducted in sterile Dulbecco's PBS (Cellgro, Mediatech; pH adjusted to 7.0) at the concentration of 5 mg ml^{-1} of recombinant α-Syn by incubating at 37 °C with constant shaking at 1,000 rpm for 7 d. The fibrils are stored at −80 °C until use.

Preparation of α-Syn from human brains

Preparation of pathological α-Syn was performed as previously described in ref. [23]. Briefly, frozen brain tissues were homogenized in HS buffer (50 mM Tris–HCl pH 7.4, 750 mM NaCl, 10 mM NaF and 5 mM EDTA) with protease and protein phosphatase inhibitors, incubated on ice for 20 min, and centrifuged at 100,000 g for 30 min. The supernatant was collected as HS fraction. The pellets were extracted one more time with HS buffer, followed by sequential extractions with 1% Triton X-100-containing HS buffer and centrifugation at 100,000 g for 30 min. The supernatant was collected as Tx fraction. HS and Tx fractions were combined together as the soluble α-Syn fraction. The pellets were re-extracted with 1% Triton X-100-containing HS buffer with 30% sucrose and 1% sarkosyl-containing HS buffer. The resulting sarkosyl-insoluble pellets were resuspended in Dulbecco's PBS by brief sonication (QSonica Microson XL-2000; 20 pulses; setting 2; 0.5 s per pulse). The amount of α-Syn in each fraction was determined by sandwich ELISAs.

IP

For the identification of PTMs, soluble α-Syn was further purified by IP as previously described in ref. [23]. Briefly, control mouse IgG (Sigma) or Syn9027, an in-house-generated antibody against α-Syn (epitope, aa130–140), were coupled to Dynabeads (Invitrogen) following the manufacturer's instructions. Soluble α-Syn from diseased or control brains was incubated with control IgG-coupled beads in Dulbecco's PBS and rotated at 4 °C overnight. The resulting supernatant was then incubated with Syn9027-coupled beads in a rotator at 4 °C overnight to capture α-Syn. The following day, the Syn9027 beads were washed three times with Dulbecco's PBS and boiled in sampling buffer and the eluted samples were stored at −80 °C until use. The single band of α-Syn monomer or the whole lane of IP eluted proteins was used for LC–MS/MS analysis.

Cell cultures and transduction

All housing and experimental procedures of mice and rats were performed according to the NIH Guide for the Care and Use of Experimental Animals and approved by the University of Pennsylvania Institutional Animal Care and Use Committee (IACUC) and the UCLA IACUC. All animals were housed in IACUC-certified animal quarters that maintain a 12 h light/12 h dark cycle at 18–23 °C with 40–60% humidity and food is available ad libitum. Primary mouse and rat neurons were prepared as previously described in ref. [35]. Misfolded α-Syn proteins were diluted in Dulbecco's PBS (without Mg^{2+} or Ca^{2+}) and sonicated using QSonica Microson XL-2000 for 60 pulses. At 10 d in vitro, primary mouse neurons were treated with PBS or sonicated misfolded α-Syn and stained at 14 d post-transduction. Rat neurons were infected with AAV expressing WT or S87E variant α-Syn at 2 d in vitro and transduced with misfolded α-Syn at 9 d in vitro and stained at 14 d post transduction. The transfection and transduction of HEK293 cells were performed as previously described in ref. [36].

To passage PFFs in HEK293 cells, 10^6 HEK293 cells were plated in a 6 cm dish, transfected to express variant α-Syn 1 d later and then transduced with PFFs or GCI-α-Syn 2 d later. Cells were collected at 3 d post-transduction with the same protocol as described for the human brain, except that 1% Triton-containing HS buffer was used in the initial extraction.

Mass spectrometry analysis

Peptides were analyzed on a QExactive HF or OrbitrapElite mass spectrometer (Thermo Fisher Scientific) coupled with an Ultimate 3000 nano UPLC system and Easy-Spray source or an Eksigent nanoLC Ultra (Sciex) and nanospray Flex ion source. Peptides were separated by reverse phase (RP)-HPLC on Easy-Spray RSLC C18 2 μm 75 μm id × 50 cm column at 50 C or 75 μm id × 15 cm Reprosil-pur 3 μm, 120 Å (Maisch) in a Nanoflex chip system (Sciex). Data were collected using data-dependent acquisition (DDA), parallel reaction monitoring (PRM) or a mixed DDA/PRM mode. In several LC–MS/MS analyses, to enhance sensitivity for low abundant peptides, the m/z and retention time (RT) for precursor ions of all identified peptides were extracted and used to construct an exclude peak list for the second runs.

Database search of the LC–MS/MS results

Peptide identification for the DDA mode was performed in MaxQuant (1.6.1.0) using human reference database from Uniprot (reviewed canonical and isoforms; downloaded on 20180104) and the search results were exported into Scaffold 4 (Proteome Software). Trypsin or AspN was selected as the digestion enzyme, and a maximum of three labeled amino acids and two missed cleavages per peptide were allowed. Fragment ion tolerance was set to 0.5 Da. The MS/MS tolerance was set at 20 ppm. The minimum peptide length was set at seven amino acids. Carbamidomethyl (+57.02146 Da) of Cys was defined as a fixed modification. In multiple search instances, several variable modifications including Ser, Thr and Tyr phosphorylation (+79.96633 Da), Glu arginylation (+156.10111 Da), O-GlcNAc (+203.07937 Da) of Thr, acetylation (+42.01056 Da)/ubiquitinylation (+114.04292 Da)/methylation (+14.01565 Da)/dimethylation (+28.03130 Da)/trimethylation (+42.04695 Da)/carboxymethylation (+58.00548 Da)/carboxyethylation (+72.02113 Da) of Lys were implemented in MaxQuant. The FDR for peptide identification was set at 1% in Scaffold 4. Peptides with scores higher than 90 and location properties higher than 0.8 by Maxquant were chosen for manual examination. All integrated peaks were manually inspected to ensure correct peak detection and integration.

Ethics approvals

All animal breeding, housing and experimental procedures were performed according to the NIH Guide for the Care and Use of Experimental Animals and approved by the University of Pennsylvania (UPenn) and the University of California, Los Angeles, IACUC. The use of postmortem brain tissue in this study has been approved by the Institutional Review Boards (IRBs) of the University of Pennsylvania and UCLA and decided as ‘exempt’ from IRB review because it is postmortem tissue.

Phosphorylation of α-Syn in vitro

WT or S87N variant α-Syn monomers were incubated with Casein Kinase I (New England Biolabs) at 37 °C overnight following the manual instructions. The phosphorylated α-Syn was analyzed by WB with antibodies against total α-Syn or S87 phosphorylated α-Syn.

Generation of Y39 phosphorylated α-Syn

To synthesize phosphorylated α-Syn, a two-piece native chemical ligation (NCL) was performed between the fragments α-Syn1-55-pY39 and α-Syn56-140. All fragments and intermediate products were purified by reverse-phase high-performance liquid chromatography (RP-HPLC) over a C4 column. α-Syn fragments were expressed from plasmid containing α-Syn fused to a polyhistidine-tagged GyrA intein from *Mycobacterium xenopi*. Following Ni-NTA affinity column purification, the intein of α-Syn56-140 was cleaved with 200 mM β-mercaptoethanol on a rotisserie overnight at room temperature to generate α-Syn56-140 with a C-terminal carboxylic acid. Removal of the N-terminal thiazolidine was carried out by reacting with 100 mM methoxyamine at pH 4 to deprotect the N-terminal cysteine for later use in ligation.

To generate α-Syn1-55 with C-terminal 2-mercaptoethanesulfonate (MES) thioester, the α-Syn1-55-intein fusion was dialyzed to remove excess imidazole before transthioesterification by stirring with 200 mM sodium 2-mercaptoethanesulfonate (MESNa) at 4 °C overnight. The purified fragment α-Syn1-55 thioester was phosphorylated by redissolving in buffer (50 mM Tris, 150 mM NaCl and pH 7.4) and reacting with 0.1 equiv c-Abl enzyme, 2 mM Mg-ATP and 5 mM $MgCl_2$. The reaction was incubated at 30 °C water bath for several hours.

To carry out NCL, α-Syn56-140 was redissolved in ligation buffer (6 M GdnHCl, 200 mM Na_2PO_4, 30 mM TCEP, 50 mM MPAA and pH 7.0). The reacting partner, α-Syn1-55-pY39-MES thioester, was added and the reaction was incubated at 37 °C with agitation at 250 rpm for several hours to overnight. The reaction was monitored by MALDI MS, and the product was reduced with 300 mM TCEP and purified by RP-HPLC. Radical desulfurization to regenerate the native alanine from the cysteine ligation handle was carried out using 50 mM radical initiator VA-044 and 10% (vol/vol) t-BuSH in an argon-purged tube at 37 °C overnight. The full-length phosphorylated α-Syn product was then purified by RP-HPLC.

Generation of S87 phosphorylated α-Syn

To synthesize α-Syn pS87, a three-piece NCL was performed between the fragments α-Syn1-84, α-Syn85-90-pS87 and α-Syn91-140. Expression and thioesterification of α-Syn1-84 MES thioester were carried out as described for α-Syn1-55. Expression and thiazolidine deprotection of α-Syn91-140 were carried out as described for α-Syn56-140.

The acyl hydrazide peptide α-Syn85-90-pS87 was made via solid phase peptide synthesis on 2-chloro-trityl resin following standard procedures. The resin was derivatized by coupling Fmoc-hydrazine, and extra sites were capped with methanol. For amino acid coupling, five equiv Fmoc-protected amino acid was activated with 4.9 equiv HBTU, 4.9 equiv HOBt, and ten equiv DIPEA and added to the deprotected peptidyl resin with

stirring for 30 min. Fmoc deprotection was done by stirring for 20 min with 20% (vol/vol) piperidine in dimethylformamide (DMF). Washes with DMF and dichloromethane (DCM) were performed between each coupling and deprotection. α-Syn85-90-pS87 was synthesized with pS at position 87 and a cysteine ligation handle at position 85. Coupling of (Fmoc-Ser(PO(OBzl)OH)-OH) was achieved by a single coupling overnight. Completion of couplings was monitored by Kaiser test. Peptide cleavage from the resin was performed by adding a few milliliters of cleavage cocktail (95% trifluoroacetic acid (TFA), 2.5% tri-isopropylsilane (TIPS) and 2.5% H_2O) and agitating for 1.5 h at room temperature. The peptide product was obtained in a 92.2% isolated yield.

To carry out NCL, α-Syn1-84-MES thioester was redissolved to a final concentration of 2 mM in ligation buffer (6 M GdnHCl, 200 mM NaH_2PO_4, 50 mM TCEP, 100 mM MPAA, pH 7.0) along with three equiv α-Syn85-90-pS87 acyl hydrazide. The reaction was incubated at 37 °C with agitation at 500 rpm for 1 h. Peptide bond formation between Gly84 thioester and Cys85 proceeded to completion within a few minutes, and the product was isolated in an 86.5% yield. The intermediate α-Syn1-90-pS87 acyl hydrazide was converted to a stable MES thioester for a methyl thioglycolate (MTG)-mediated second NCL and in situ desulfurization, following the strategy described in previous publication[1]. α-Syn1-pS87 acyl hydrazide was redissolved in low pH NCL buffer (6 M GdnHCl, 200 mM NaH_2PO_4 and pH 3.0) to a final concentration of 1 mM and chilled to −15 °C in an ice-salt bath. Hydrazide to azide conversion was carried out using ten equiv $NaNO_2$ and agitating by magnetic stirring for 15 min. The sample was supplemented with 100 equiv MESNa as a neutral buffered solution, and the mixture was allowed to warm to room temperature and adjusted to pH 7.0. The product was supplemented with TCEP to a final concentration of ~40 mM before purification by RP-HPLC using a C4 column.

To carry out the second NCL, α-Syn1-pS87 MES thioester was dissolved together with three equiv ligation partner α-Syn91-140 in NCL buffer pH 7 to a final concentration of 1.5 mM. A hundred equiv MTG was added from a stock dilution in NCL buffer pH 7.0. The reaction was supplemented with TCEP to a final concentration of 40 mM, adjusted to pH 7.0 and incubated at 37 °C with agitation at 500 rpm for 4h. To regenerate the native Ala85 and Ala91 from the cysteine ligation handles, radical desulfurization was carried out without intermediary purification. The NCL reaction mixture was diluted with buffer pH 7.0 so that the final protein concentration was 0.4 mM. The mixture was incubated with 20 mM radical initiator VA-044, 10% (vol/vol) *t*-BuSH, and 250 mM TCEP in an argon-purged tube at 37 °C overnight and purified by RP-HPLC. Overall steps, α-Syn pS87 was obtained in 61.6% isolated yield.

Each reaction was monitored by MALDI MS and by analytical HPLC on a 1260 Infinity Series HPLC using a Jupiter C4 column (Agilent Technologies). All fragments and intermediate products were purified over a C4 column on a Varian preparative HPLC equipped with a fraction collector and diode array detector (Agilent Technologies). Water + 0.1% TFA (solvent A) and acetonitrile + 0.1% TFA (solvent B) were used as the mobile phase in HPLC.

In vitro seeding assay

Pathological α-Syn (LB-α-Syn, GCI-α-Syn or PFF) was mixed with phosphorylated α-Syn monomers at the following concentration: 10 ng μl^{-1} pathological α-Syn + 95 ng μl^{-1} pY39 α-Syn monomer + 95 ng μl^{-1} pS87 α-Syn monomer. PFFs were mixed with insoluble proteins from normal brains to mimic the contaminating proteins in LB-α-Syn and GCI-α-Syn. The pathological α-Syn was sonicated for 30 cycles using the Bioruptor Plus sonicator from Diagenode (30 s on and 30 s off in each cycle at high power) before mixing with the monomers. The total volume for each reaction was 50 µl. The mixture was shaken at 37 °C for 4 weeks at 1,000 rpm for fibrilization.

Immunocytochemistry

Cells were fixed with 4% PFA containing 1% Triton X-100 for 15 min to remove soluble proteins. Fixed coverslips or plates were blocked with 3% BSA and 3% FBS for 1 h at room temperature and incubated with specific primary antibodies at 4 °C overnight followed by staining with secondary antibodies and DAPI for 2 h at room temperature. The stained cells in plates were scanned with an IN Cell Analyzer 2200. The stained coverslips were scanned into digital format with a Lamina scanner (Perkin Elmer). Digitalized plates and coverslips were then used for quantification. For HDTA extraction, cells were extracted with 1% HDTA for 15 min and then fixed in 4% PFA for 15 min before staining.

Sandwich ELISA

α-Syn ELISA has been performed as previously described in ref. [2]. Syn9027 or HuA have been used as capture antibodies and MJF-R1, HuA or Syn211 were used as the reporter antibodies. Finally, plates were read at 450 nm on a Molecular Devices Spectramax M5 plate reader.

In solution digestion for mass spectrometry

Samples were precipitated by the addition of acetone/trichloroacetic acid (8 volumes per 1 volume). The resulting pellet was solubilized and digested with the iST kit (PreOmics GmbH) per manufacturer protocol[3]. Briefly, the resulting pellet was solubilized, reduced and alkylated by addition of sodium deoxycholate buffer containing Tris 2-carboxyethyl phosphine hydrochloride (TCEP) and 2-chloroacetamide and heated to 95 °C for 10 min. Proteins were enzymatically hydrolyzed for 1.5 h at 37 °C by addition of AspN (Sigma) or trypsin (Promega). The resulting peptides were desalted, dried by vacuum centrifugation and reconstituted in 0.1% TFA (J.T. Baker) containing iRT peptides (Biognosys).

In gel digestion for mass spectrometry

Samples were run into a 10% Bis-Tris 1.0 gel (Invitrogen) and stained with colloidal Coomassie. Samples were excised and cut into 1 mm^3 cubes[44], destained with 50% methanol per 1.25% acetic acid, reduced with 5 mM DTT (Dithiothreitol) (Thermo) and alkylated with 20 mM iodoacetamide (Sigma). Gel pieces were then washed with 20 mM ammonium bicarbonate (Sigma) and dehydrated with acetonitrile (Fisher). Trypsin (Promega) or AspN (Sigma) (5 ng ml^{-1} in 20 mM ammonium bicarbonate) was added to the gel pieces and proteolysis was allowed to proceed overnight at 37 °C. Proteolysis was

stopped by the addition of 0.3% TFA. The supernatant was removed and placed in a 0.5 ml tube. Peptides were extracted with 50% acetonitrile. Extracts were combined and the volume was reduced by vacuum centrifugation. Samples were subjected to stage tip cleanup[5], dried by vacuum centrifugation and reconstituted in 0.1% TFA.

IMAC for phosphopeptide enrichment

Peptides from each sample were freeze-dried and dissolved in 75% acetonitrile per 0.1% TFA. The metal affinity chromatography (IMAC) beads (PHOS-select iron affinity beads; Sigma, P9740-5ML) were washed two times 500 µl with buffer W/E (30% acetonitrile per 250 mM acetic acid) at 8,000 rcf for 1 min[6]. Peptide mixtures were incubated with 10 µl of 25% IMAC beads for 1 h at 1,000 rpm at RT. The enriched phosphopeptides on the IMAC beads were loaded onto a prewashed 96-well glass fiber filter plate (Phenomenex, AF0-8265). The flow-through of the unbound IMAC peptides was kept for acetylated peptide enrichment. The IMAC beads were washed sequentially under vacuum with two times 400 µl W/E buffer; 80% acetonitrile per 0.1% TFA; and 30% acetonitrile/water. Phosphorylated peptides were eluted two times 400 µl with elution buffer (400 mM ammonium hydroxide per 30% acetonitrile) after 1 min incubation each. The eluted peptides were collected with a new LoBind Plate 96-well collection plate (Eppendorf, 0030 504.305).

Immunoaffinity enrichment for acetylated peptides

To enrich acetylated peptides from the unbound IMAC peptides, the unbound peptides were lyophilized and dissolved in IAP buffer (50 mM MOPS, 50 mM NaCl, 10 mM Na2HPO4, pH ~7.2) according to the manufacturer's instruction. The PTMScan Acetyl-Lysine Motif (Ac-K) Immunoaffinity Beads were purchased from Cell Signaling (Prod, 13416). The beads were washed three times with 1 ml IAP, ~5 µl 100% beads were used for each sample for the immunoaffinity enrichment[7] under end-end mixing for 1 h at 4 °C. The beads were then washed with two times 1 ml IAP, 1× IAP plus 0.05% RapiGest SF (Waters) surfactant, followed by three times 1 ml PBS washes; the lysine-acetylated peptides were eluted with two times 40 µl 0.15% TFA. The eluted acetylated peptides were desalted via Oasis HLB µElution plate 30 µM (Waters). The enriched peptides from both IMAC and acetylated immunoaffinity were dried via speedvac for overnight, and they were dissolved in 0.1% TFA/water including iRT peptides. Both eluates were combined to a final volume of 8 µl for LC–MS analysis.

Supplementary Material

Refer to Web version on PubMed Central for supplementary material.

Acknowledgements

We thank Quantitative Proteomics Resource Core of School of Medicine at the University of Pennsylvania and Proteomics Core at Children's Hospital of Philadelphia (CHOP) for performing the LC–MS/MS analysis. We thank S. Seeholzer, L. Spruce, H. Ding, H. Fazelinia and H. Lee (from CHOP) for helping with LC–MS/MS experiments. We thank D. Riddle for providing primary neurons, L. Romero for helping with quantification and all the other members of the Center for Neurodegenerative Disease Research for their support. We thank Lucy Ruoxi Shi for helping with the cartoon illustration of this work. This work was supported by NIH/NINDS Udall Center under grant NS53488 (to V.M.-Y.L.), NIA under grant U19 AG062418 (Center on Alpha-Synuclein Strains in Alzheimer's Disease and Related Dementias) (to V.M.-Y.L.), NIH/NINDS R01-NS103873 to E.J.P. (to V.M.-Y.L.),

NIH/NINDS R01-NS128964 (to C.P.), CurePSP grant 672-2020-12 (to C.P.), the Ofer Nimerovsky Family Fund (to V.M.-Y.L.), the Jeff and Anne Keefer Fund (to V.M.-Y.L.) and the MSA Coalition Seed Grant (to C.P. and V.M.-Y.L.). The funders had no role in study design, data collection and analysis, decision to publish or preparation of the manuscript.

Data availability

Peptide identification was performed in MaxQuant (1.6.1.0) using human reference database from Uniprot (reviewed canonical and isoforms; downloaded on 1 January 2018) and the search results were exported into Scaffold 4 (Proteome Software). The mass spectrometry proteomics data have been deposited to the ProteomeXchange Consortium via the PRIDE[37] partner repository with the dataset identifier PXD037994. Figure 3 and Supplementary Tables 4-8 are associated with LC–MS/MS data. Source data are provided with this paper.

References

1. Lippa CF et al. Lewy bodies contain altered α-synuclein in brains of many familial Alzheimer's disease patients with mutations in presenilin and amyloid precursor protein genes. Am. J. Pathol 153, 1365–1370 (1998). [PubMed: 9811326]
2. Spillantini MG et al. α-Synuclein in Lewy bodies. Nature 388, 839–840 (1997). [PubMed: 9278044]
3. Tu PH et al. Glial cytoplasmic inclusions in white matter oligodendrocytes of multiple system atrophy brains contain insoluble α-synuclein. Ann. Neurol 44, 415–422 (1998). [PubMed: 9749615]
4. Luk KC et al. Pathological α-synuclein transmission initiates Parkinson-like neurodegeneration in nontransgenic mice. Science 338, 949–953 (2012). [PubMed: 23161999]
5. Kordower JH, Chu Y, Hauser RA, Freeman TB & Olanow CW Lewy body-like pathology in long-term embryonic nigral transplants in Parkinson's disease. Nat. Med 14, 504–506 (2008). [PubMed: 18391962]
6. Li JY et al. Lewy bodies in grafted neurons in subjects with Parkinson's disease suggest host-to-graft disease propagation. Nat. Med 14, 501–503 (2008). [PubMed: 18391963]
7. Braak H & Tredici KD Neuroanatomy and pathology of sporadic Parkinson's disease. Adv. Anat. Embryol. Cell Biol 201, 1–119 (2009). [PubMed: 19230552]
8. Jucker M & Walker LC Propagation and spread of pathogenic protein assemblies in neurodegenerative diseases. Nat. Neurosci 21, 1341–1349 (2018). [PubMed: 30258241]
9. Guo JL & Lee VM Cell-to-cell transmission of pathogenic proteins in neurodegenerative diseases. Nat. Med 20, 130–138 (2014). [PubMed: 24504409]
10. Barrett PJ & Timothy Greenamyre J Post-translational modification of α-synuclein in Parkinson's disease. Brain Res. 1628, 247–253 (2015). [PubMed: 26080075]
11. Schmid AW, Fauvet B, Moniatte M & Lashuel HA α-Synuclein post-translational modifications as potential biomarkers for Parkinson disease and other synucleinopathies. Mol. Cell. Proteom 12, 3543–3558 (2013).
12. Burai R, Ait-Bouziad N, Chiki A & Lashuel HA Elucidating the role of site-specific nitration of α-synuclein in the pathogenesis of Parkinson's disease via protein semisynthesis and mutagenesis. J. Am. Chem. Soc 137, 5041–5052 (2015). [PubMed: 25768729]
13. Dikiy I et al. Semisynthetic and in vitro phosphorylation of α-synuclein at Y39 promotes functional partly helical membrane-bound states resembling those induced by PD mutations. ACS Chem. Biol 11, 2428–2437 (2016). [PubMed: 27356045]
14. Hejjaoui M et al. Elucidating the role of C-terminal post-translational modifications using protein semisynthesis strategies: α-synuclein phosphorylation at tyrosine 125. J. Am. Chem. Soc 134, 5196–5210 (2012). [PubMed: 22339654]
15. Levine PM et al. α-Synuclein O-GlcNAcylation alters aggregation and toxicity, revealing certain residues as potential inhibitors of Parkinson's disease. Proc. Natl Acad. Sci. USA 116, 1511–1519 (2019). [PubMed: 30651314]

16. Mahul-Mellier AL et al. c-Abl phosphorylates α-synuclein and regulates its degradation: implication for α-synuclein clearance and contribution to the pathogenesis of Parkinson's disease. Hum. Mol. Genet 23, 2858–2879 (2014). [PubMed: 24412932]
17. Oueslati A, Schneider BL, Aebischer P & Lashuel HA Polo-like kinase 2 regulates selective autophagic α-synuclein clearance and suppresses its toxicity in vivo. Proc. Natl Acad. Sci. USA 110, E3945–E3954 (2013). [PubMed: 23983262]
18. Paleologou KE et al. Phosphorylation at S87 is enhanced in synucleinopathies, inhibits α-synuclein oligomerization, and influences synuclein-membrane interactions. J. Neurosci 30, 3184–3198 (2010). [PubMed: 20203178]
19. Negro A, Brunati AM, Donella-Deana A, Massimino ML & Pinna LA Multiple phosphorylation of α-synuclein by protein tyrosine kinase Syk prevents eosin-induced aggregation. FASEB J. 16, 210–212 (2002). [PubMed: 11744621]
20. Chen L et al. Tyrosine and serine phosphorylation of α-synuclein have opposing effects on neurotoxicity and soluble oligomer formation. J. Clin. Investig 119, 3257–3265 (2009). [PubMed: 19855133]
21. Marotta NP et al. α-Synuclein from patient Lewy bodies exhibits distinct pathological activity that can be propagated in vitro. Acta Neuropathol. Commun 9, 188 (2021). [PubMed: 34819159]
22. Schweighauser M et al. Structures of α-synuclein filaments from multiple system atrophy. Nature 585, 464–469 (2020). [PubMed: 32461689]
23. Peng C et al. Cellular milieu imparts distinct pathological α-synuclein strains in α-synucleinopathies. Nature 557, 558–563 (2018). [PubMed: 29743672]
24. Pan B, Rhoades E & Petersson EJ Chemoenzymatic semisynthesis of phosphorylated α-synuclein enables identification of a bidirectional effect on fibril formation. ACS Chem. Biol 15, 640–645 (2020). [PubMed: 32065743]
25. Pan B et al. Effects of glutamate arginylation on α-synuclein: studying an unusual post-translational modification through semisynthesis. J. Am. Chem. Soc 142, 21786–21798 (2020). [PubMed: 33337869]
26. Oueslati A, Paleologou KE, Schneider BL, Aebischer P & Lashuel HA Mimicking phosphorylation at serine 87 inhibits the aggregation of human α-synuclein and protects against its toxicity in a rat model of Parkinson's disease. J. Neurosci 32, 1536–1544 (2012). [PubMed: 22302797]
27. Brahmachari S et al. Activation of tyrosine kinase c-Abl contributes to α-synuclein-induced neurodegeneration. J. Clin. Investig 126, 2970–2988 (2016). [PubMed: 27348587]
28. de Oliveira RM et al. The mechanism of sirtuin 2-mediated exacerbation of α-synuclein toxicity in models of Parkinson's disease. PLoS Biol. 15, e2000374 (2017). [PubMed: 28257421]
29. Vicente Miranda H et al. Glycation potentiates α-synuclein-associated neurodegeneration in synucleinopathies. Brain 140, 1399–1419 (2017). [PubMed: 28398476]
30. Marotta NP et al. O-GlcNAc modification blocks the aggregation and toxicity of the protein α-synuclein associated with Parkinson's disease. Nat. Chem 7, 913–920 (2015). [PubMed: 26492012]
31. Wang J et al. Protein arginylation targets α-synuclein, facilitates normal brain health and prevents neurodegeneration. Sci. Rep 7, 11323 (2017). [PubMed: 28900170]
32. Zhao J et al. α-Synuclein arginylation in the human brain. Transl. Neurodegener 11, 20 (2022). [PubMed: 35395956]
33. Morris M et al. Tau post-translational modifications in wild-type and human amyloid precursor protein transgenic mice. Nat. Neurosci 18, 1183–1189 (2015). [PubMed: 26192747]
34. Narasimhan S et al. Pathological tau strains from human brains recapitulate the diversity of tauopathies in nontransgenic mouse brain. J. Neurosci 37, 11406–11423 (2017). [PubMed: 29054878]
35. Volpicelli-Daley LA et al. Exogenous α-synuclein fibrils induce Lewy body pathology leading to synaptic dysfunction and neuron death. Neuron 72, 57–71 (2011). [PubMed: 21982369]
36. Luk KC et al. Exogenous α-synuclein fibrils seed the formation of Lewy body-like intracellular inclusions in cultured cells. Proc. Natl Acad. Sci. USA 106, 20051–20056 (2009). [PubMed: 19892735]

37. Perez-Riverol Y et al. The PRIDE database resources in 2022: a hub for mass spectrometry-based proteomics evidence. Nucleic Acids Res. 50, D543–D552 (2022). [PubMed: 34723319]

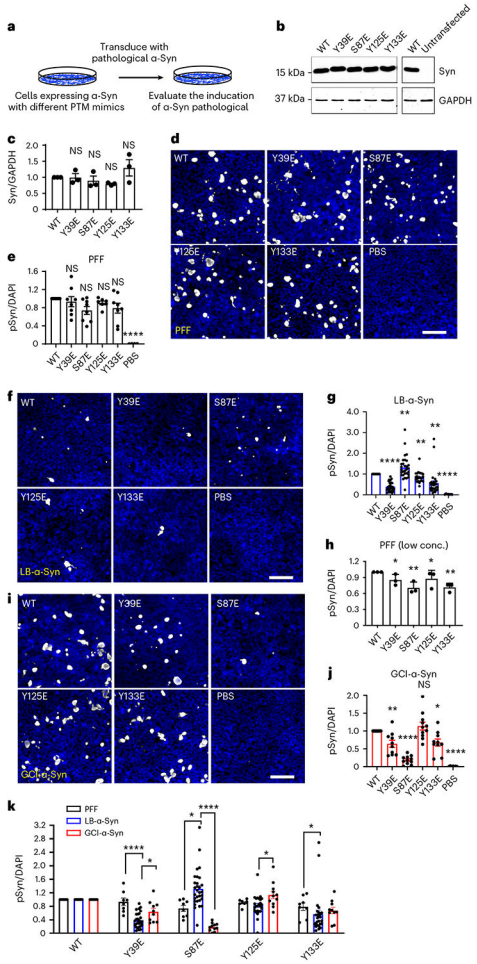

Fig. 1 | Soluble α-Syn phosphorylation modulates pathological α-Syn amplification.

a, Schematic representation of experiment design. **b**, α-Syn variants show similar expression levels. (Repeated three times.) **c**, Densitometric quantification of α-Syn variants for experiments in **b**. (n = 3 different samples. Y39E, P = 0.9763; S87E, P = 0.724; Y125E, P = 0.0512 and Y133E, P = 0.724). **d**, Cells expressing α-Syn variants were transduced with α-Syn PFFs (40 ng per well). The induced α-Syn pathologies were stained with anti-pS129 α-Syn antibody (81A). (Repeated > 5 times.) **e**, Quantification of α-Syn pathology for experiments in **d**. (WT, n = 10; Y39E, S87E and Y133E, n = 8; Y125E, n = 7 and PBS, n = 4. Three different batches of PFF were tested. Y39E, P = 0.5633; S87E, P = 0.052; Y125E, P = 0.0883; Y133E, P = 0.120 and PBS, P < 0.0001). **f**, Cells expressing α-Syn variants were transduced with LB-α-Syn (4 ng per well) and stained with 81A. (Repeated > 7 times.) **g**, Quantification of α-Syn pathology for experiments in **f**. (PBS, n = 7; WT, n = 33; Y39E, n = 27; S87E, n = 30; Y125E, n = 25 and Y133E, n = 26. LB-α-Syn from eight cases were tested. Y39E, P < 0.0001; S87E, P = 0.0018; Y125E, P = 0.0018; Y133E, P = 0.0015 and PBS, P < 0.0001). **h**, Cells expressing α-Syn variants were transduced with low amount of α-Syn PFFs (4 ng per well) and the induced α-Syn pathology are quantified. (n = 3 different PFFs. Y39E, P = 0.0105; S87E, P = 0.0034; Y125E, P = 0.0313 and Y133E, P = 0.0034). **i**, Cells expressing α-Syn variants were transduced with GCI-α-Syn (40 pg per

well) and stained with 81A. (Repeated > 7 times.) **j**, Quantification of α-Syn pathology for experiments in i. (WT, $n = 14$; Y39E and Y133E, $n = 10$; S87E and Y125E, $n = 11$ and PBS, $n = 7$. GCI-α-Syn from six cases was tested. Y39E, $P = 0.0092$; S87E, $P < 0.0001$; Y125E, $P = 0.2446$; Y133E, $P = 0.0113$ and PBS, $P < 0.0001$). **k**, Combining the data in **e**, **g** and **j**. (The n are the same as in **e**, **g** and **j**. Y39E LB versus PFF, $P < 0.0001$; Y39E LB versus GCI, $P = 0.0359$; S87E LB versus PFF, $P = 0.0368$; S87E LB versus GCI, $P < 0.0001$; Y125E LB versus GCI, $P = 0.0297$ and Y133E LB versus PFF, $P = 0.0300$). Results are shown as mean ± s.e.m. Statistics in **c, e, g, h** and **j** are one sample *t*-test (for normally distributed data) or one sample Wilcoxon test (for non-normally distributed data) against one. Statistics in **k** are one-way ANOVA with Tukey's multiple comparison test (for normally distributed data) or Kruskal–Wallis test with Dunn's multiple comparison test (for non-normally distributed data) in each variant group. The P values in **c, e, g, h** and **j** are FDR corrected. *$P < 0.05$; **$P < 0.01$; ***$P < 0.001$; ****$P < 0.0001$; NS, not significant. Scale bar, 100 μm.

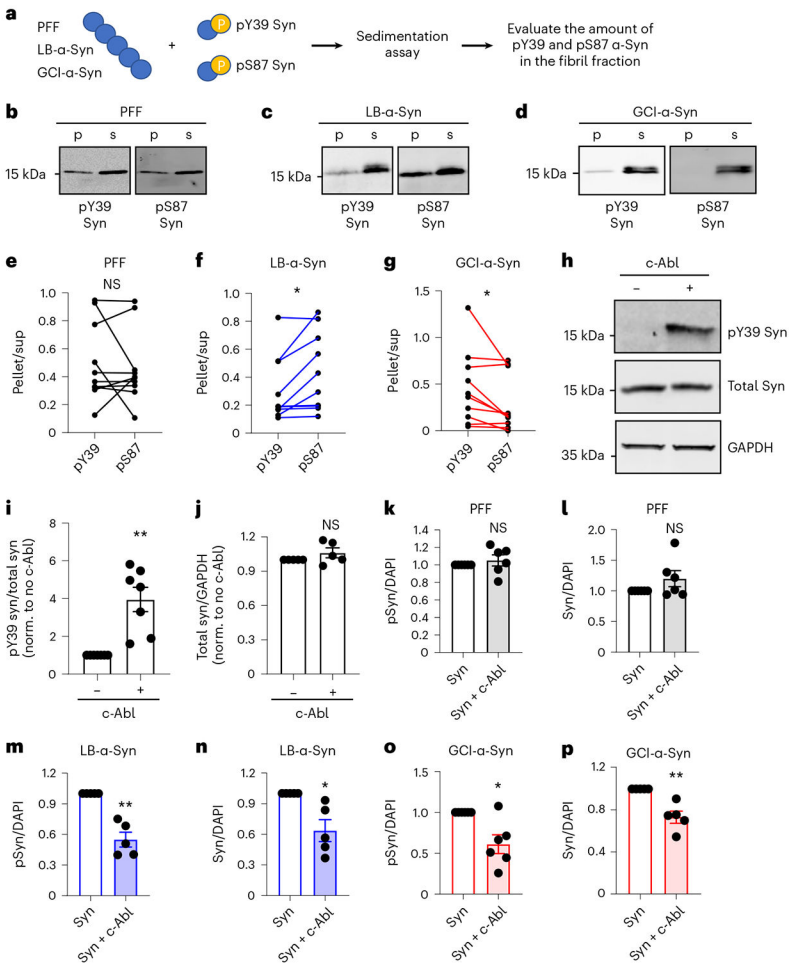

Fig. 2 | Soluble α-Syn phosphorylation modulates GCI-α-Syn and LB-α-Syn amplification.
a, Schematic diagram showing the seeding assay. Equal amounts of pY39 and pS87 α-Syn monomer mixture were seeded with PFF, LB-α-Syn or GCI-α-Syn. After fibrilization, the amount of pS87 and pY39 α-Syn in the fibril fraction were analyzed by sedimentation assay and WB, to evaluate which monomer is more easily seeded by pathological α-Syn. **b–d**, Representative WB results with antibodies against pY39 or pS87 α-Syn for experiment in **a**. P, pellet; s, supernatant in the sedimentation assay. (Repeated nine times for **b** and **c**, ten times for **d**.) **e–g**, Quantification results for experiments in **b–d**. **e**, PFF seed pY39 or pS87 α-Syn monomer equally ($n = 9$ different samples, $P = 0.9414$). **f**, LB-α-Syn preferentially seeds pS87 over pY39 α-Syn ($n = 9$ different samples, $P = 0.0176$). **g**, GCI-α-Syn preferentially seeds pY39 over pS87 α-Syn ($n = 10$ different samples, $P = 0.0195$). **h**, WT α-Syn was expressed in cells with or without c-Abl. pY39 α-Syn, total α-Syn and glyceraldehyde 3-phosphate dehydrogenase (GAPDH) were evaluated by WB (repeated > 5 times). **i**, Densitometric quantification of pY39 α-Syn versus total α-Syn for experiments in **h** ($n = 7$ different samples, $P = 0.0038$). **j**, Densitometric quantification of total α-Syn versus GAPDH for experiments in **h**. ($n = 5$ different samples, $P = 0.2366$). **k**,**l**, α-Syn was expressed in cells with or without c-Abl and seeded by PFF. The cells were stained with anti-pS129 α-Syn to evaluate α-Syn pathology (**k**) or extracted with 1%HDTA and stained

with anti total α-Syn to evaluate insoluble α-Syn (**l**). (n = 6, three different PFF were tested; **k**, P = 0.4552; **l**, P = 0.1891). **m**,**n**, Similar to **k** and **l**, but seeded with LB-α-Syn. (n = 5, LB-α-Syn from three cases were tested; **m**, P = 0.0034; **n**, P = 0.0275). **o**,**p**, Similar to **k** and **l**, but seeded with GCI-α-Syn (n = 6 for **o**, n = 5 for **p**, GCI-α-Syn from three cases were tested; **o**, P = 0.0193; **p**, P = 0.0096). Results are shown as mean ± s.e.m. Statistics in **e**, **f** and **g** are two-tailed Wilcoxon matched-pairs signed rank test t-test. Statistics in **i–p** are one sample t-test against 1. *P < 0.05; **P < 0.01; ***P < 0.001; NS, not significant.

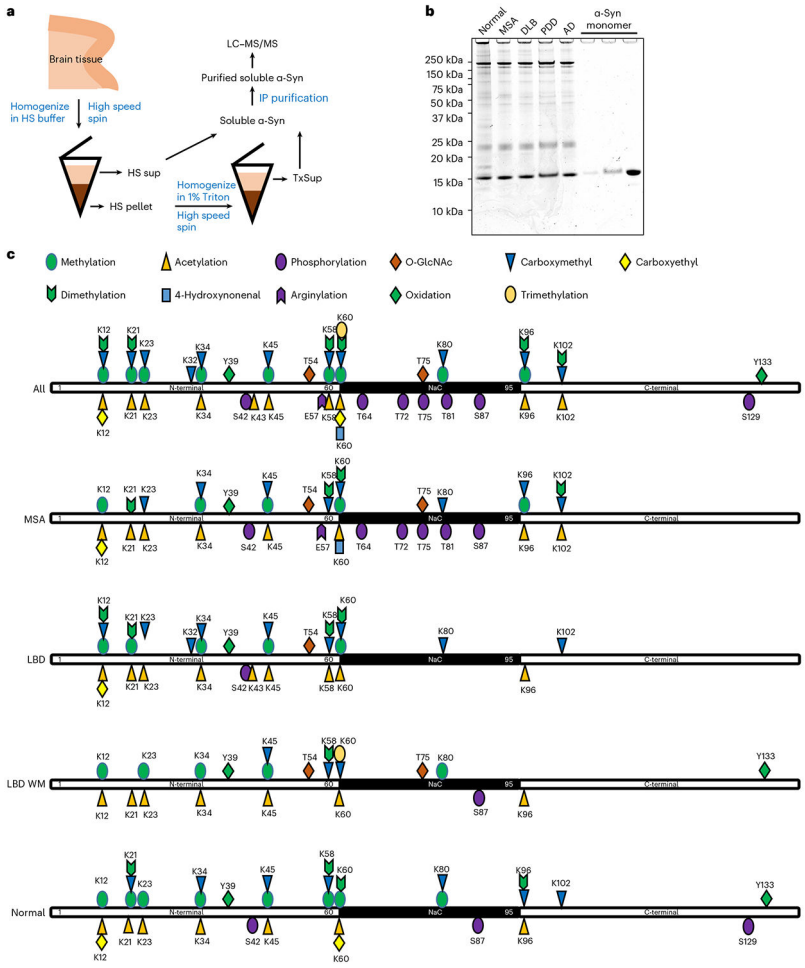

Fig. 3 | Systematically identify PTMs on soluble α-Syn from different α-synucleinopathies. **a**, Schematic diagram showing the purification of soluble α-Syn from disease brains. **b**, IP-purified soluble α-Syn from various α-synucleinopathy and control brains and recombinant α-Syn monomers were resolved on 12% Bis-Tris gel and stained with Coomassie Blue. (Repeated three times.) **c**, Summary of PTMs identified on soluble α-Syn purified from different α-synucleinopathy and control brains. WM, white matter.

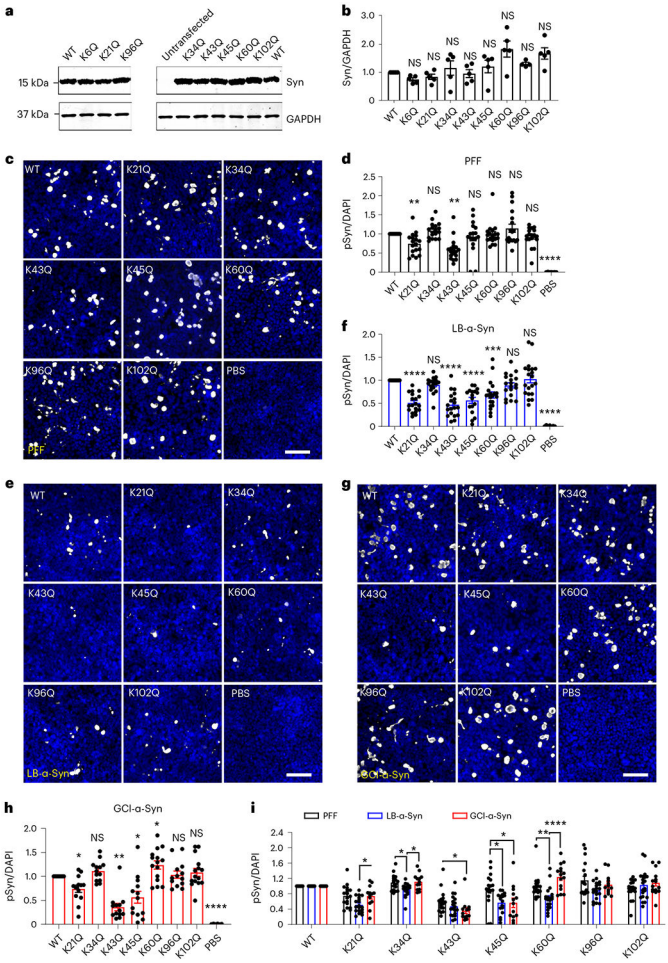

Fig. 4 | Soluble α-Syn acetylation modulates pathological α-Syn amplification.

a, Acetylation mimetic α-Syn variants showed similar expression levels in cells. (Repeated five times.) **b**, Densitometric quantification of α-Syn for experiment in **a**. ($n = 4$ for K96Q, $n = 5$ for the other groups; K6Q, $P = 0.0544$; K21Q, $P = 0.268$; K34Q, $P = 0.658$; K43Q, $P = 0.772$; K45Q, $P = 0.539$; K60Q, $P = 0.088$; K96Q, $P = 0.0544$; K102Q, $P = 0.0776$.) **c**, Cells expressing α-Syn variants were transduced with α-Syn PFFs (40 ng per well) and stained with anti-pS129 α-Syn (81A). (Repeated > 7 times.) **d**, Quantification of α-Syn pathology for **c**. (PBS, $n = 7$; WT, $n = 21$; K21Q, K43Q, K60Q, K96Q and K102Q, $n = 18$; K34Q and K45Q, $n = 17$. Four different PFF were tested. K21Q, $P = 0.0029$; K34Q, $P = 0.1768$; K43Q, $P = 0.0012$; K45Q, $P = 0.543$; K60Q, $P = 0.2264$; K96Q, $P = 0.6397$; K102Q, $P = 0.543$; PBS, $P < 0.0001$). **e**, Cells expressing α-Syn variants were transduced with LB-α-Syn (4 ng per well) and stained with 81A. (Repeated > 7 times.) **f**, Quantification of α-Syn pathology for **e** (PBS, $n = 7$; WT, $n = 25$; K21Q, K43Q and K96Q, $n = 19$; K34Q and K45Q, $n = 17$; K60Q and K102Q, $n = 20$. LB-α-Syn from eight cases were tested. K21Q, $P < 0.0001$; K34Q, $P = 0.0539$; K43Q, $P < 0.0001$; K45Q, $P < 0.0001$; K60Q, $P = 0.0002$; K96Q, $P = 0.0783$; K102Q, $P = 0.7282$; PBS, $P < 0.0001$). **g**, Cells expressing α-Syn variants were transduced with GCI-α-Syn (40 pg per well) and stained with 81A. (Repeated > 7 times). **h**, Quantification of α-Syn pathology for **g**. (PBS, $n = 6$; WT, $n = 18$; K21Q, K34Q, K43Q,

K45Q and K96Q, $n = 13$; K60Q and K102Q, $n = 15$. GCI-α-Syn from six cases were tested. K21Q, $P = 0.0114$; K34Q, $P = 0.103$; K43Q, $P = 0.002$; K45Q, $P = 0.0112$; K60Q, $P = 0.0245$; K96Q, $P = 0.6425$; K102Q, $P = 0.362$; PBS, $P < 0.0001$). **i**, Combining the data in **d**, **f** and **h**. (The n is the same as **d**, **f** and **h**. K21Q PFF versus LB, $P = 0.0184$; K21Q LB versus GCI, $P = 0.0385$; K34Q PFF versus LB, $P = 0.0234$; K34Q LB versus GCI, $P = 0.0174$; K43Q PFF versus GCI, $P = 0.0130$; K45Q PFF versus LB, $P = 0.0248$; K45Q PFF versus GCI, $P = 0.0379$; K60Q PFF versus LB, $P = 0.0088$; K60Q LB versus GCI, $P < 0.0001$) Results shown as mean ± s.e.m. N represents biological replicates. Statistics in **b**, **d**, **f** and **h** are one sample t-test (for normally distributed data) or one sample Wilcoxon test (for non-normally distributed data) against one. Statistics in i are one-way ANOVA with Tukey's multiple comparison test (for normally distributed data) or Kruskal–Wallis test with Dunn's multiple comparison test (for non-normally distributed data) in each variant group. The P values in **b**, **d**, **f** and **h** are FDR corrected. $*P < 0.05$; $**P < 0.01$; $***P < 0.001$; $****P < 0.0001$; NS, not significant. Scale bar, 100 μm.

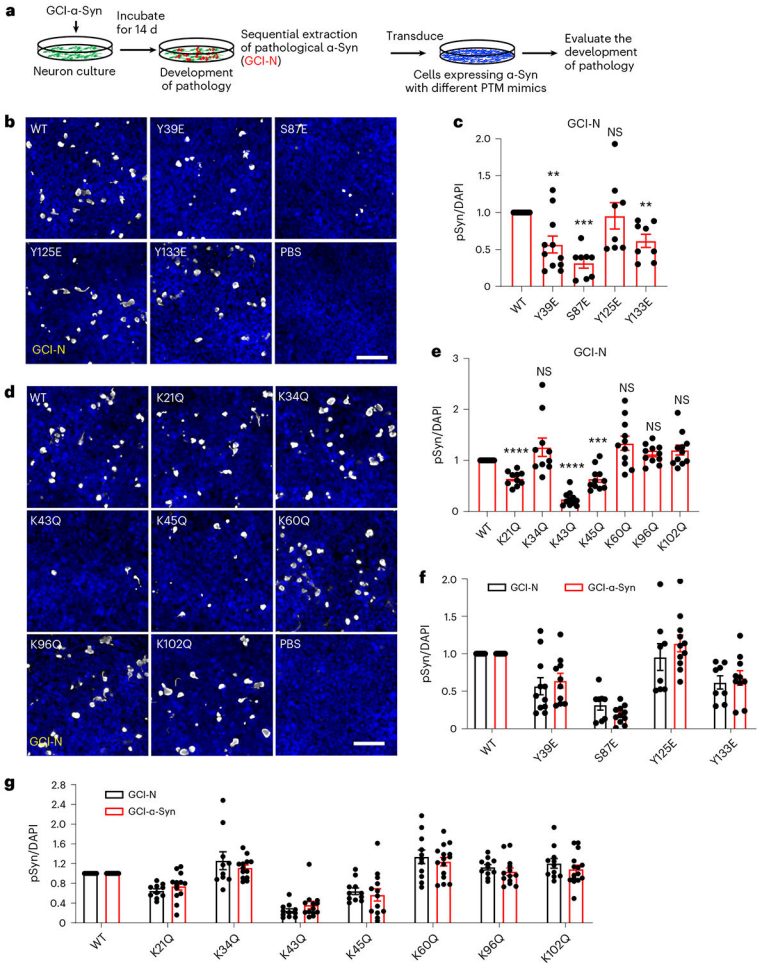

Fig. 5 | The effect of soluble α-Syn PTMs on pathological α-Syn transmission is conformation dependent.

a, Schematic representation showing the passaging of GCI-α-Syn in primary neurons. **b**, HEK293 cells expressing phosphorylation mimetic α-Syn variants were transduced with GCI-α-Syn that was passaged in primary neurons (GCI-N) (40 pg per well) and stained with anti-pS129 α-Syn antibody (81A). (Repeated seven times.) **c**, Quantification of α-Syn pathology (pSyn normalized with total DAPI counts) for experiments in **b**. (n = 11 for WT and Y39E, n = 8 for S87E, Y125E and Y133E. Seven different GCI-N were tested. Y39E, P = 0.0079; S87E, P = 0.00011; Y125E, P = 0.8138; Y133E, P = 0.0072). **d**, HEK293 cells expressing acetylation mimetic α-Syn variants were transduced with GCI-N and stained with 81A. (Repeated ten times.) **e**, Quantification of α-Syn pathology for experiments in **d**. (n = 10 for K21Q and K34Q, n = 11 for the other groups. Seven different GCI-N were tested. K21Q, P < 0.0001; K34Q, P = 0.3223; K43Q, P < 0.0001; K45Q, P = 0.0007; K60Q, P = 0.0623; K96Q, P = 0.0638; K102Q, P = 0.0714.) **f,g**, Both phosphorylation and acetylation of soluble α-Syn showed similar effects on the transmission of GCI-N and GCI-α-Syn. (For GCI-α-Syn group in **f**, n = 11 for WT, n = 7 for Y39E, n = 8 for S87E, Y125E and Y133E. For GCI-N group in **f**, n = 10 for WT and Y39E, n = 7 for S87E, Y125E and Y133E. For GCI-α-Syn group in **g**, n = 18 for WT, n = 13 for K21Q, K34Q, K43Q, K45Q and K96Q, n = 15 for K60Q and K102Q. For GCI-N group in **g**, n = 11 for

WT, $n = 10$ for K21Q and K34Q, $n = 11$ for K43Q, K45Q, K60Q, K96Q and K102Q.) Results are shown as mean ± s.e.m. N represents biological replicates. Statistics in **c** and **e** are one sample *t*-test (for normally distributed data) or one sample Wilcoxon test (for non-normally distributed data) against one. Statistics in **f** and **g** are unpaired two-tailed *t*-test (for normally distributed data; if variances are substantially different, perform Welch's correction) or Mann–Whitney test (for non-normally distributed data) in each variant group. The P values in **c** and **e** are FDR corrected. *$P < 0.05$; ****$P < 0.0001$; NS, not significant. Scale bar, 100 μm.

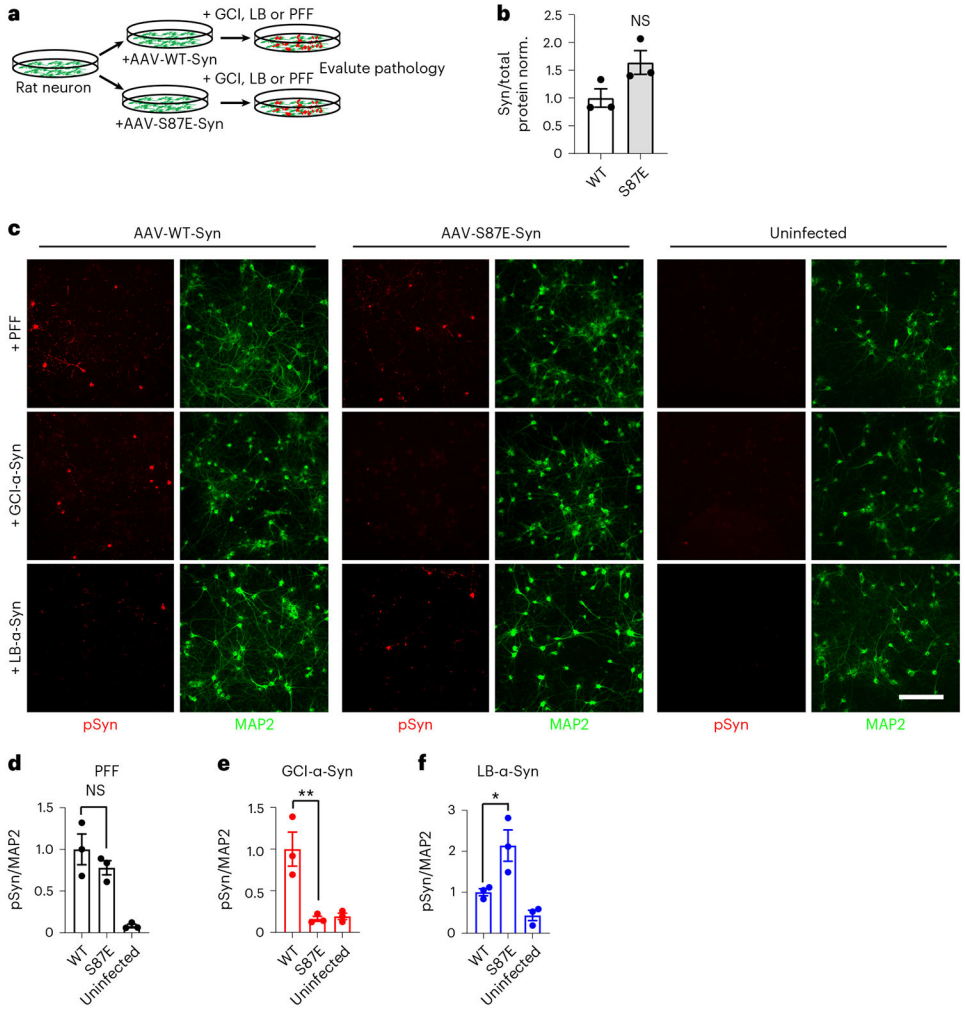

Fig. 6 | PTMs of soluble α-Syn modify the spreading of pathological α-Syn in primary neurons. **a**, Schematic representation: rat primary neurons were infected with AAV to express either WT or S87E variant α-Syn and then transduced with GCI-α-Syri (40 pg per well), α-Syn PFFs (40 ng per well) or LB-α-Syn (4 ng per well). **b**, WT and S87E α-Syn show similar expression levels in rat primary neurons as measured by ELISA. ($n = 3$ different samples, $P = 0.100$). **c**, As described in **a**, transduced neurons were extracted with 1% Triton X-100 and stained with antibodies against α-Syn phosphorylated at S129 (pSyn) and MAP2. S87E α-Syn dramatically blocked the seeding ability of GCI-α-Syn and increased the seeding ability of LB-α-Syn but did not have significant effects on α-Syn PFF. There is very little α-Syn pathology in uninfected groups. (Repeated three times) **d–f**, Quantification of the amount of α-Syn pathology (pSyn normalized with total MAP2 signal) for experiments described in **c**. ($n = 3$, three different PFFs, LB-α-Syn and GCI-α-Syn from different cases were tested here. WT versus S87E, $P = 0.4355$ for **d**, $P = 0.0067$ for **e**, $P = 0.0338$ for **f**. Results are shown as mean ± s.e.m. Statistics in **b** are unpaired, two-tailed Mann–Whitney test. Statistics in **d**, **e** and **f** are one-way ANOVA with Tukey's multiple comparison test. *$P < 0.05$; **$P < 0.01$; NS, not significant. Scale bar, 200 μm.

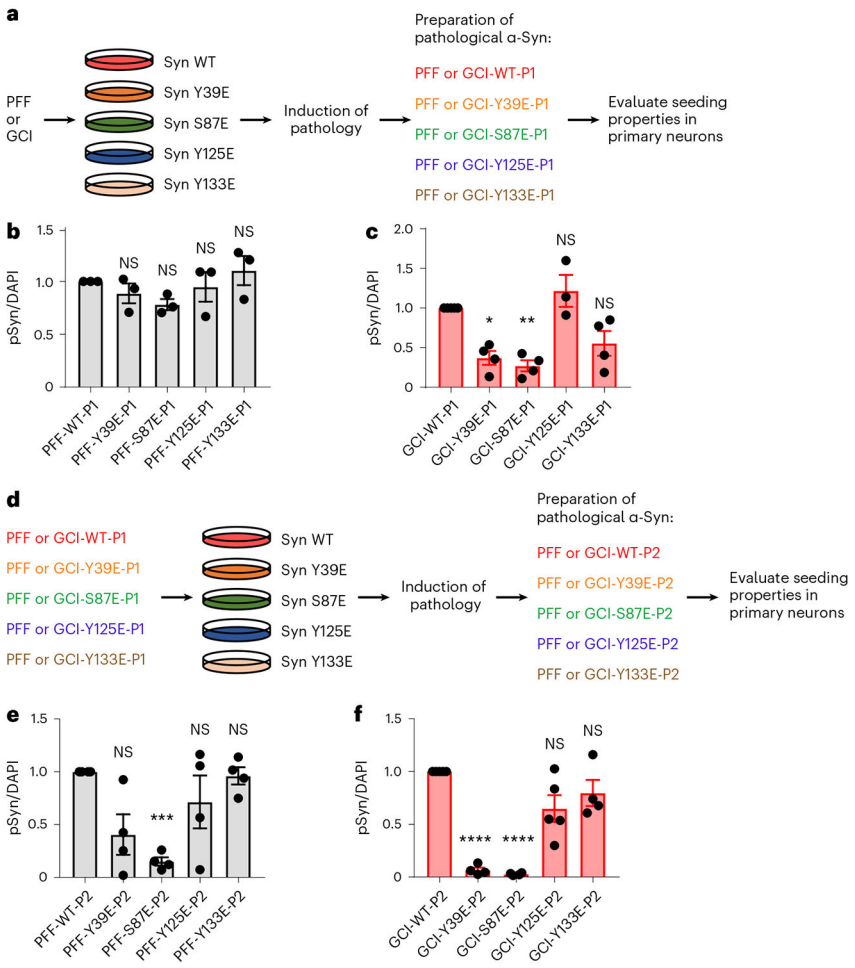

Fig. 7 | PTMs on soluble α-Syn modify the seeding properties of pathological α-Syn.

a, Schematic representation: HEK293 cells expressing α-Syn variants with different phosphorylation mimics were transduced with α-Syn PFFs or GCI-α-Syn. The induced insoluble pathological α-Syn proteins were enriched by sequential extraction with 1% Triton X-100 and 1% sarkosyl-containing buffers. **b**, Mice primary neurons were transduced with α-Syn PFFs (40 ng per well) that had been passaged in cells expressing different α-Syn variants. After induction of α-Syn pathology, cells were extracted with buffer containing 1% Triton X-100 to remove soluble proteins and stained with antibodies against the phosphorylated S129 α-Syn and MAP2. The amount of α-Syn pathology was quantified as the total amount of pSyn normalized with MAP2. Passaging α-Syn variants with different phosphorylation mimics once did not change the seeding properties of α-Syn PFFs. ($n = 3$ different batches of passaged PFF for all groups. PFF-Y39E-P1 $P = 0.7018$, PFF-S87E-P1 $P = 0.2092$, PFF-Y125E-P1 $P > 0.9999$ and PFF-Y133E-P1 $P = 0.71$.) **c**, Similar to **b**, mouse primary neurons were transduced with GCI-α-Syn (40 pg per well) that had been passaged once in different α-Syn variants. Passaging in cells expressing Y39E and S87E variant α-Syn dramatically reduced the seeding ability of the GCI-α-Syn strain. ($n = 5$ for GCI-WT-P1, $n = 4$ for GCI-Y39E-P1, GCI-S87E-P1 and GCI-Y133E-P1, $n = 3$ for GCI-Y125E-P1. n represents biological replicates. Three different batches of passaged GCI-

α-Syn were tested here with some batches being tested multiple times. GCI-Y39E-P1 P = 0.011, GCI-S87E-P1 P = 0.0072, GCI-Y125E-P1 P = 0.3962 and GCI-Y133E-P1 P = 0.086.) **d**, Schematic representation showing passaging of GCI-α-Syn and PFFs in cells expressing α-Syn variants with different phosphorylation mimics for a second round of amplification (P2). **e**, Evaluating the seeding ability of α-Syn PFFs (40 ng per well) that had been passaged in variant α-Syn for two rounds showed that continuous passaging in Y39E and S87E variant α-Syn leads to a dramatic reduction of the seeding ability of these PFFs. (n = 4, three different batches of passaged PFF were tested here with one batch being tested twice. PFF-Y39E-P2 P = 0.107, PFF-S87E-P2 P = 0.0008, PFF-Y125E-P2 P = 0.4492 and PFF-Y133E-P2 P = 0.6639.) **f**, Similar to the experiments described in **e**, continuous passaging of GCI-α-Syn in Y39E and S87E variant α-Syn led to a dramatic reduction of the seeding ability of GCI-α-Syn (40 pg per well). (n = 5 for GCI-WT-P2 and GCI-Y125E-P2, n = 4 for GCI-Y39E-P2, GCI-S87E-P2 and GCI-Y133E-P2. n represents biological replicates. Three different batches of passaged GCI-α-Syn were tested here with some batches being tested multiple times. GCI-Y39E-P2 P < 0.0001, GCI-S87E-P2 P < 0.0001, GCI-Y125E-P2 P = 0.0672 and GCI-Y133E-P2 P = 0.1986.) Results are shown as mean ± s.e.m. Statistics are one sample t-test (for normally distributed data) or one sample Wilcoxon test (for non-normally distributed data) against one. The P values are FDR corrected. *P < 0.05; **P < 0.01; ***P < 0.001; ****P < 0.0001; NS, not significant.